doi:10.1093/brain/awy129 BRAIN 2018: 141; 1–4 | e55

BRAIN
A JOURNAL OF NEUROLOGY

LETTER TO THE EDITOR

Expanding the phenotype of *TRAK1* mutations: hyperekplexia and refractory status epilepticus

Shira Sagie,[1,*] Tally Lerman-Sagie,[1,2,3,*] Snezana Maljevic,[4,5] Keren Yosovich,[6] Katja Detert,[4] Seo-Kyung Chung,[7] Mark I. Rees,[7] Holger Lerche[4] and Dorit Lev[1,3,8]

*These authors contributed equally to this work.

1 Sackler School of Medicine, Tel-Aviv University, Tel-Aviv, Israel
2 Pediatric Neurology Unit, Wolfson Medical Center, Holon, Israel
3 Metabolic-Neurogenetic Clinic, Wolfson Medical Center, Holon, Israel
4 Department of Neurology and Epileptology, Hertie Institute for Clinical Brain Research, University of Tübingen, Tübingen, Germany
5 Florey Institute of Neuroscience and Mental Health, The University of Melbourne, Parkville, Victoria, Australia
6 Molecular Laboratory, Wolfson Medical Center, Holon, Israel
7 Institute of Life Sciences, Swansea University Medical School, Swansea University, UK
8 Institute of Medical Genetics, Wolfson Medical Center, Holon, Israel

Correspondence to: Tally Lerman-Sagie, MD
Pediatric Neurology Unit
Wolfson Medical Center
Holon, Israel
E-mail: tally.sagie@gmail.com

Sir,

We read with great interest, the article by Barel *et al.* (2017) presenting the first cases of disease causing mutations in the trafficking protein, kinesin binding 1 gene (*TRAK1*). They described six patients from three unrelated consanguineous families of Arab descent, who suffered from a fatal encephalopathy and carried the same homozygous truncating mutation c.287-2A>C in *TRAK1*.

TRAK1 is a kinesin adaptor protein that has several putative roles. Gilbert *et al.* (2006) described a hypertonic mouse model with mutated *Trak1*. These mice had lower $GABA_A$ receptors in their CNS, especially in lower motor neurons, thus implicating *Trak1* as a crucial regulator of $GABA_A$ receptor homeostasis.

Webber *et al.* (2008) found that TRAK1 interacts with Hrs (hepatocyte-growth-factor-regulated tyrosine kinase substrate) and regulates endosome to lysosome trafficking.

A possible role in neuronal inhibition was suggested following the identification of a susceptibility locus for childhood absence epilepsy in the 3p23-p14 locus that includes *TRAK1* in a genome wide linkage analysis (Chioza *et al.*, 2009).

The most studied role of TRAK1 is in mitochondrial trafficking, as TRAK1 links mitochondria to kinesin motor proteins together with the Rho GTPase, Miro. A recent study suggested that TRAK1 dependent mitochondrial trafficking differs between young and mature neurons. In hippocampal and cortical neurons TRAK1 traffics mitochondria mainly in axons, but in young neurons it does so both in axons and dendrites (Loss and Stephenson, 2017). Another role of TRAK1 is in mitochondrial fusion via interaction with mitofusins. Depletion of TRAK1 was found to cause mitochondrial fragmentation (Lee *et al.*, 2017). Barel *et al.* (2017) demonstrated that the mutation in *TRAK1*, damaged mitochondrial distribution, membrane potential and motility.

A study on genetic causes for intellectual disability (Anazi *et al.*, 2017), found mutations in *TRAK1* in two families. The patients presented with: neonatal respiratory distress, seizures, delayed myelination and brain atrophy.

Advance Access publication May 26, 2018

In this letter, we describe the identification of a homozygous missense variant in the *TRAK1* gene in two siblings of unrelated Ashkenazi-Jewish parents who presented with hyperekplexia and fatal refractory status epilepticus. The full clinical presentation of this new syndrome was described in 2004 (Lerman-Sagie *et al.*, 2004). The study was approved by the Helsinki committee of the Israeli Health Department. Written informed consents were obtained from all subjects and their respective guardians.

The patients, a girl (Patient 1) and a boy (Patient 2), were born 4 years apart after a normal pregnancy and delivery to healthy parents. On their first day of life they presented with increased muscle tone and an exaggerated startle response to tactile stimulation. Motor development was mildly delayed but social, fine motor, and language development were normal. The mother described a tendency to 'startle much too often' since birth; the babies would become suddenly rigid, particularly during baths (Supplementary Videos 1 and 2 of both patients). Exam during the first year of life revealed hypotonia, hyperekplexia, and hyperreflexia, with no dysmorphic features. The boy was treated with clonazepam since birth to ameliorate the hyperekplexia and prevent seizures. Following a febrile illness (the girl at the age of 18 months, and the boy at 12 months) they experienced a tonic-clonic seizure that progressed into status epilepticus. Seizures were not controlled despite adequate anti-epileptic treatment and trials of steroids and intravenous immunoglobulin (IVIG). The patients expired following refractory status epilepticus after 17 and 12 days, respectively. An evaluation before seizure onset, revealed normal MRI, EEG, and metabolic testing. In Patient 1, a muscle biopsy was normal; a brain MRI during the status epilepticus demonstrated a hyperintense lesion in the right thalamus and bilateral tissue loss in the Sylvian fissure; and a mtDNA duplication was identified by Southern blot analysis. An autopsy revealed normal muscle and mitochondria, and brain tissue showed increased microglia in the cortex and hippocampus, mild astrocytic proliferation in the hippocampal region, and perivascular mononuclear infiltrates.

Mutations in genes known to be associated with hyperekplexia or related to glycine or GABA receptors [*GLRA1*, *GLRB*, *GPHN*, *ARHGEF9*, GlyT1 (*SLC6A9*), GlyT2 (*SLC6A5*), *GABARAP* and *GABARAPL1*] were sequenced and excluded in this family thus it was suggested that these patients had a new autosomal recessive syndrome.

We sought to identify the disease-causing variants by homozygosity mapping (the parents' ancestors were both from the same region in Romania) combined with whole exome sequencing. Whole genome single nucleotide polymorphism (SNP) analysis revealed few regions of shared homozygosity; the largest regions were Ch.3:36.624.933–42.503.035 and Ch.10:92.280.193–96.115.639. Exome sequencing was performed on Patient 1; variants were filtered based on an allele frequency <0.01 according to online databases: dbSNP, 1000G, ExAC, gnomAD. Likely pathogenicity was assessed if the variant was truncating (splicing or non-sense), missense or an in-frame indel. Missense and in-frame indels were considered if they were predicted to be pathogenic by online prediction tools: PolyPhen-2, SIFT and MutationTaster. We found two non-synonymous coding SNPs in the homozygous region in chromosome 3 predicting the amino acid exchanges p.L329P in TRAK1, and p.R798Q in the Villin-like protein (VILL). In the chromosome 10 region, there was no unreported SNP. Apart from these variants no additional homozygous or compound heterozygous unreported variants were identified. We analysed the variants in both genes in all family members and found that the two variants segregated with the disease (Fig. 1A). Confirmation and familial segregation were performed using direct Sanger sequencing (3100 Genetic Analyzer Applied Biosystems). The affected children were found to be homozygous and the parents and one healthy child heterozygous (Fig. 1A and B) for the c.986T>C mutation in the *TRAK1* gene (NM_001042646) and for the c.2393G>A in the *VILL* gene (NM_015873). SIFT and PolyPhen-2 predicted the p.L329P variant in TRAK1 to be probably damaging, and the p.R798Q variant in VILL to be tolerable or benign in the main transcripts of the gene. In the Genome Aggregation Database (http://gnomad.broadinstitute.org), the heterozygous allele count is 7/244 764 alleles for the p.L329P in the *TRAK1* gene and 70/274 990 alleles for the p.R798Q variant in the *VILL* gene, with zero homozygous cases for both. The seven variants present in the gnomAD database for TRAK1 were only detected in the Ashkenazi-Jewish population (7/9808 alleles). Further *TRAK1* variants were not found in seven additional patients with hyperekplexia and epilepsy belonging to a large cohort of patients with hyperekplexia.

The TRAK1 and not the VILL variant was considered responsible for the patient's severe neurological involvement for the following reasons. The *Trak1* mouse model manifests a similar phenotype to our patients with hypertonia and jerky movements (Gilbert *et al.*, 2006), and demonstrates the involvement of TRAK1 in $GABA_A$ receptor trafficking. In addition, the TRAK1 protein is expressed in the CNS (the human protein atlas https://www.proteinatlas.org). The p.L329P variant, affecting a highly conserved amino acid (Fig. 1C), was predicted to probably damage the protein structure and is very rare in the Genome Aggregation data.

In contrast, a mouse model, the oligotriche mouse (*olt*/*olt* homozygous mutant) with a 234 kbp deletion including the *VILL* gene orthologue in mice, *Vill* (villin like), and additional genes, does not have a neurological phenotype. These mice have alopecia and male infertility, attributed to the *Plcd1* gene included in the deleted region (Runkel *et al.*, 2008). The *VILL* gene, part of the villin/gelsolin family, which is suggested to participate in actin bundling, has not been described as disease causing and is transcribed and expressed mainly in the gut and not in the CNS. The variant found in our patients was not predicted to damage the protein and is 10 times more prevalent than the variant found in the *TRAK1* gene.

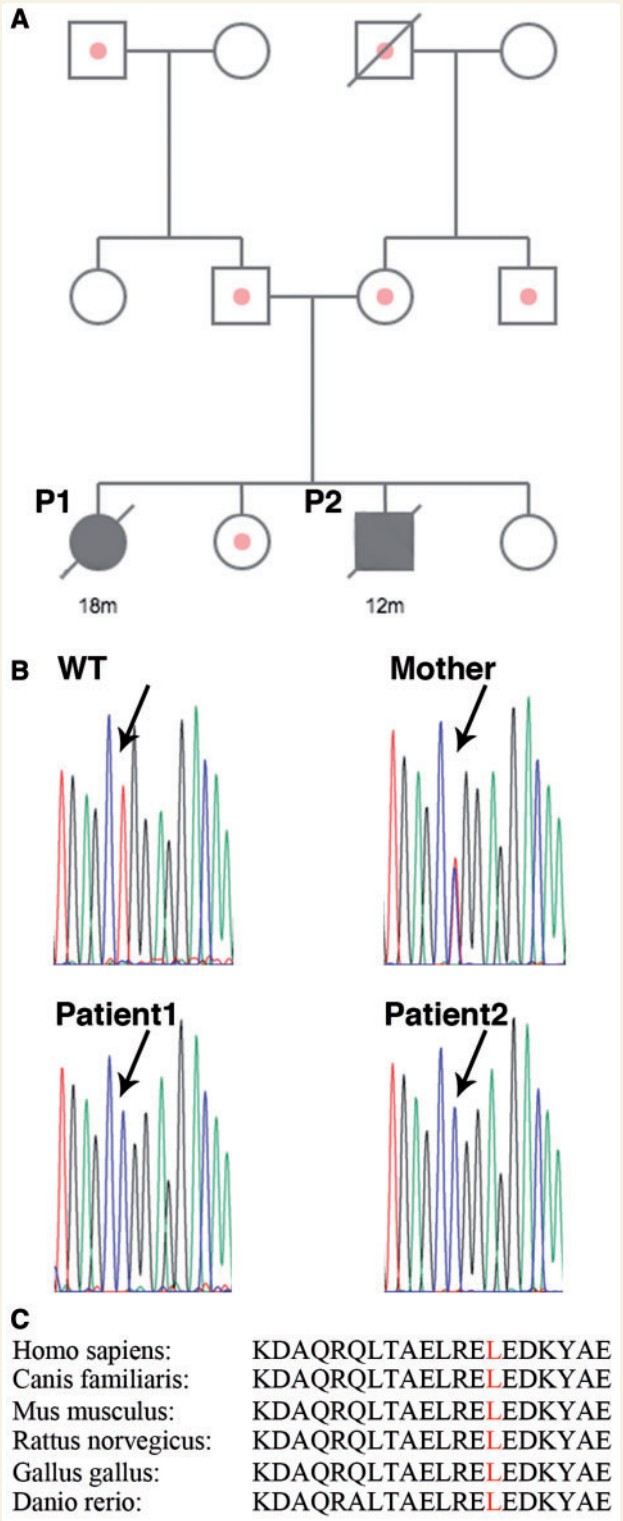

Figure 1 Family pedigree, identified mutations and evolutionary conservation of the altered amino acid in the *TRAK1* gene. (**A**) Pedigree of the family, the last child was born after identification of the mutation. (**B**) Sanger confirmation analysis of the missense variant L329P in the *TRAK1* gene (NM_001042646 c.986 T>C) Carrier heterozygosity in the parents and homozygosity in the affected individual were confirmed. (**C**) Evolutionary conservation of the *TRAK1* gene.

We functionally tested the p.L329P variant in TRAK1 using a *Xenopus laevis* oocyte expression system. Co-expression of the TRAK1 wild-type or mutant proteins with the most abundant $GABA_A$ receptor comprised $\alpha_1\beta_2\gamma_2$ subunits revealed no difference in the recorded GABA-evoked responses using two-microelectrode voltage clamping (data not shown). This suggests that the interaction of wild-type or mutant TRAK1 protein with $GABA_A$ receptors does not differentially affect trafficking, function or stability of these $GABA_A$ complexes in *Xenopus* oocytes. Other functional assays, exploring the effects of this variant on $GABA_A$ receptors and mitochondrial function, will therefore be necessary to understand the disease mechanism.

Hyperekplexia is a rare neurogenetic disorder characterized by neonatal hypertonia and exaggerated startle reflex after sudden tactile, auditory or visual stimuli accompanied by temporary generalized stiffness and falls. It is mostly dominantly inherited and caused by mutations in the glycine receptors α and β subunit genes (*GLRA1* and *GLRB*) that facilitate fast-response, inhibitory neurotransmission in the spinal cord and brainstem. Additional mutations were found in other postsynaptic proteins of glycinergic synapses as in GPHN, collybistin and ARHGEF9 (Harvey *et al.*, 2008). In contrast to most patients with hyperekplexia, our patients exhibited hypertonicity only during the neonatal period, with decreased tone in infancy. Seizures are infrequently described in patients with hyperekplexia (Harvey, 2004; Zeydan *et al.*, 2017); however, refractory status epilepticus has not been described.

Our patients' clinical presentation is different from that described by Barel *et al.* since the most dominant feature was congenital hyperekplexia. In addition, their development was only mildly delayed, and they did not have epilepsy until they succumbed to refractory status epilepticus, at the age of 12 and 18 months. In contrast, the patients reported by Barel *et al.* (2017) presented during infancy (age 1 month to 19 months) with myoclonus, they had global developmental delay, epilepsy started in the first 2 years of life, developmental regression occurred after the onset of epilepsy, and in addition they all developed spasticity.

Hyperekplexia was only described in one of the patients from the Barel series and another was described as having an exaggerated startle response. All other patients were described with early onset myoclonus. The *Trak1* mouse manifested 'jerky movements', which could be the equivalent of hyperekplexia or myoclonus in mice.

Barel *et al.* (2017) demonstrated that TRAK1-deficient fibroblasts showed irregular distribution, altered motility, reduced membrane potential, and diminished respiration of mitochondria. At the molecular level, the variant resulted in the formation of an early termination codon and nonsense mediated decay, suggesting that TRAK1 interaction with trafficking or mitochondrial transport would be lacking in the homozygous carriers.

Conversely, the variant in our patients (p.L329P) is located close to the Hrs interaction site involved in endosome to lysosome trafficking and far from the part of the protein responsible for generation of mitochondrial complexes (Stephenson, 2014). Therefore, we suggest that the pathomechanism involved in our patients, producing a different phenotype, may not be related to mitochondrial dysfunction but rather to dysregulation of endosome to lysosome trafficking of neuronal inhibitory proteins. Further research is needed to elucidate the exact mechanism.

Acknowledgements

This paper is in memory of Dr Esther Leshinsky-Silver who found the gene in 2011 and enabled the birth of a healthy child in this family.

Funding

The generous support of Rabbi Bochner of the Bonei Olam organization is acknowledged.

Supplementary material

Supplementary material is available at *Brain* online.

References

Anazi S, Maddirevula S, Salpietro V, Asi YT, Alsahli S, Alhashem A, et al. Expanding the genetic heterogeneity of intellectual disability. Hum Genet 2017; 136: 1419–29.

Barel O, Malicdan MCV, Ben-Zeev B, Kandel J, Pri-Chen H, Stephen J, et al. Deleterious variants in TRAK1 disrupt mitochondrial movement and cause fatal encephalopathy. Brain 2017; 140: 568–81.

Chioza BA, Aicardi J, Aschauer H, Brouwer O, Callenbach P, Covanis A, et al. Genome wide high density SNP-based linkage analysis of childhood absence epilepsy identifies a susceptibility locus on chromosome 3p23-p14. Epilepsy Res 2009; 87: 247–55.

Gilbert SL, Zhang L, Forster ML, Iwase T, Soliven B, Donahue LR, et al. Trak1 mutation disrupts $GABA_A$ receptor homeostasis in hypertonic mice. Nat Genet 2006; 38: 245–50.

Harvey K. The GDP-GTP exchange factor collybistin: an essential determinant of neuronal gephyrin clustering. J Neurosci 2004; 24: 5816–26.

Harvey RJ, Topf M, Harvey K, Rees MI. The genetics of hyperekplexia: more than startle! Trends Genet 2008; 24: 439–47.

Lee CA, Chin LS, Li L. Hypertonia-linked protein Trak1 functions with mitofusins to promote mitochondrial tethering and fusion. Protein Cell 2017, in press. doi: 10.1007/s13238-017-0469-4.

Lerman-Sagie T, Watemberg N, Vinkler C, Fishhof J, Leshinsky-Silver E, Lev D. Familial hyperekplexia and refractory status epilepticus: a new autosomal recessive syndrome. J Child Neurol 2004; 19: 522–5.

Loss O, Stephenson FA. Developmental changes in trak-mediated mitochondrial transport in neurons. Mol Cell Neurosci 2017; 80: 134–47.

Runkel F, Aubin I, Simon-Chazottes D, Büssow H, Stingl R, Miething A, et al. Alopecia and male infertility in oligotriche mutant mice are caused by a deletion on distal chromosome 9. Mamm Genome 2008; 19: 691–702.

Stephenson FA. Revisiting the TRAK family of proteins as mediators of $GABA_A$ receptor trafficking. Neurochem Res 2014; 39: 992–6.

Webber E, Li L, Chin LS. Hypertonia-associated protein Trak1 is a novel regulator of endosome-to-lysosome trafficking. J Mol Biol 2008; 382: 638–51.

Zeydan B, Gunduz A, Demirbilek V, Dervent A. Visually evoked startle response in a patient with epilepsy: a case report and review of the literature. Neurocase 2017; 23: 79–81.

Published in final edited form as:
Nat Genet. 2015 April ; 47(4): 393–399. doi:10.1038/ng.3239.

De novo loss- or gain-of-function mutations in *KCNA2* cause epileptic encephalopathy

Steffen Syrbe[#1], Ulrike B.S. Hedrich[#2], Erik Riesch[#3,4,5], Tania Djémié[#6,7], Stephan Müller[2], Rikke S. Møller[8,9], Bridget Maher[10,11], Laura Hernandez-Hernandez[10,11], Matthis Synofzik[12,13], Hande S. Caglayan[14], Mutluay Arslan[15], José M. Serratosa[16,17], Michael Nothnagel[18], Patrick May[19], Roland Krause[19], Heidrun Löffler[2], Katja Detert[2], Thomas Dorn[5], Heinrich Vogt[5], Günter Krämer[5], Ludger Schöls[12,13], Primus E. Mullis[20], Tarja Linnankivi[21], Anna-Elina Lehesjoki[22,23,24], Katalin Sterbova[25], Dana C. Craiu[26,27], Dorota Hoffman-Zacharska[28], Christian M. Korff[29], Yvonne G. Weber[2], Maja Steinlin[30], Sabina Gallati[4], Astrid Bertsche[1], Matthias K. Bernhard[1], Andreas Merkenschlager[1], Wieland Kiess[1], EuroEPINOMICS RES consortium, Michael Gonzalez[32], Stephan Züchner[32], Aarno Palotie[33,34,35], Arvid Suls[6,7], Peter De Jonghe[6,7,36], Ingo Helbig[37,38], Saskia Biskup[3], Markus Wolff[39], Snezana Maljevic[2], Rebecca Schüle[12,13,30], Sanjay M. Sisodiya[10,11], Sarah Weckhuysen[6,7,41], Holger Lerche[2,41], and Johannes R. Lemke[1,4,40,41]

[1]Department of Women and Child Health, Hospital for Children and Adolescents, University of Leipzig, Leipzig, Germany. [2]Department of Neurology and Epileptology, Hertie Institute for Clinical Brain Research, University of Tübingen, Tübingen, Germany. [3]Center for Genomics and Transcriptomics (CeGaT) GmbH, Tübingen, Germany. [4]Division of Human Genetics, University Children's Hospital Inselspital, Bern, Switzerland. [5]Swiss Epilepsy Center, Zürich, Switzerland. [6]Neurogenetics group, Department of Molecular Genetics, VIB, Antwerp, Belgium. [7]Laboratory of Neurogenetics, Institute Born-Bunge, University of Antwerp, Antwerp, Belgium. [8]Danish Epilepsy Center, Dianalund, Denmark [9]Institute for Regional Health Services, University of Southern Denmark, Odense, Denmark. [10]Department of Clinical and Experimental Epilepsy, University College London Institute of Neurology, Queen Square, London, WC1N 3BG, UK [11]Epilepsy Society, Chalfont-St-Peter, Bucks, SL9 0RJ, UK. [12]Department of Neurodegenerative Diseases, Hertie Institute for Clinical Brain Research, University of Tübingen, Tübingen, Germany.

Correspondence: Johannes R. Lemke, MD Institut für Humangenetik Universität Leipzig Philipp-Rosenthal-Str.55 D-04103 Leipzig, Germany Tel.: +49-341-97-23800 Fax: +49-341-97-23819 johannes.lemke@medizin.uni-leipzig.de Holger Lerche, MD Abteilung Neurologie mit Schwerpunkt Epileptologie Hertie Institut für Klinische Hirnforschung Universität Tübingen Hoppe-Seyler-Str. 3 D-72076 Tübingen, Germany Tel.: +49-7071-29-80442 Fax: +49-7071-29-4488 holger.lerche@uni-tuebingen.de.
[31]Full lists of members and affiliations appear at the end of the paper.
[41]These authors jointly directed the work

Author contributions Study design: S.S., U.B.S.H., S.W., H.Le., J.R.L.; subject ascertainment and phenotyping: S.S., E.R., R.S.M., B.M., L.H.H., H.S.C., M.A., J.M.S., T.Do., H.V., G.K., M.Sy., L.S., P.E.M., T.L., A.-E.L., K.S., D.C., D.H.-Z., C.M.K., Y.G.W., M.St., S.G., A.B., M.K.B., A.M., W.K., A.P., A.S., P.D.J., I.H., S.B., M.W., S.M.S., S.W., H.Le., J.R.L., EuroEPINOMICS; mutation and CNV analysis: E.R., T.Dj., B.M., L.H.H., R.S., M.G., S.Z., A.S., P.D.J., S.B., S.M.S., S.W., H.Le., J.R.L.; statistical analysis: M.N., P.M., R.K., H.Le., J.R.L.; functional analysis: U.B.S.H., S.Mü., H.Lö., K.D., S.Ma., H.Le.; interpretation of data: S.S., U.B.S.H., M.W., S.Ma., S.M.S., S.W., H.Le., J.R.L.; writing manuscript: S.S., U.B.S.H., T.Dj., M.S., M.N., P.M., S.Ma., S.M.S., S.W., H.Le., J.R.L.; revising manuscript: all authors.

Competing financial interests The authors declare no competing financial interests.

Accession codes Data of the panel sequencing cohort is accessible on the GEM.app browser as "EuroEPINOMICS CH/DK cohort". Data of trio exome sequencing cohorts is accessible on the GEM.app browser as "RES EE trio sequencing" cohort.

[13]German Research Center for Neurodegenerative Diseases (DZNE), Tübingen, Germany [14]Department of Molecular Biology and Genetics, Bogazici University, Istanbul, Turkey. [15]Gulhane Military Medical School, Division of Child Neurology, Ankara, Turkey. [16]Neurology Lab and Epilepsy Unit, Department of Neurology, IIS — Fundación Jiménez Díaz, UAM, Madrid, Spain [17]Centro de Investigación Biomédica en Red de Enfermedades Raras (CIBERER), Madrid, Spain. [18]Cologne Center for Genomics, University of Colgone, Cologne, Germany [19]Luxembourg Centre for Systems Biomedicine (LCSB), University of Luxembourg, Esch-sur-Alzette, Luxembourg [20]Division of Pediatric Endocrinology, University Children's Hospital Inselspital, Bern, Switzerland. [21]Pediatric Neurology, Children's Hospital, University of Helsinki and Helsinki University Hospital, Helsinki, Finland. [22]Folkhälsan Institute of Genetics, Helsinki, Helsinki, Finland. [23]Neuroscience Center, University of Helsinki, Helsinki, Finland [24]Research Program's Unit, Molecular Neurology, University of Helsinki, Helsinki, Finland [25]Child Neurology Department, 2nd Faculty of Medicine, Charles University, Motol Hospital, Prague, Czech Republic. [26]Pediatric Neurology Clinic II, Department of Neurology, Pediatric Neurology, Psychiatry, and Neurosurgery, "Carol Davila" University of Medicine, Sector 4, Bucharest, Romania. [27]Pediatric Neurology Clinic, "Professor Doctor Alexandru Obregia" Clinical Hospital, Sector 4, Bucharest, Romania. [28]Department of Medical Genetics, Institute of Mother and Child, Warsaw, Poland. [29]Child and Adolescent Department, Pediatric Neurology, University Hospitals, Geneva, Switzerland. [30]Division of Neuropediatrics, University Children's Hospital Inselspital, Bern, Switzerland. [32]Dr. JT MacDonald Department for Human Genetics, Hussman Institute for Human Genomics, University of Miami, Miami, USA [33]Institute for Molecular Medicine Finland, University of Helsinki, Helsinki, Finland [34]Wellcome Trust Sanger Institute, Wellcome Trust Genome Campus, Hinxton, UK. [35]Psychiatric & Neurodevelopmental Genetics Unit, Department of Psychiatry, Massachusetts General Hospital, Boston, MA, 02114, USA [36]Department of Neurology, Antwerp University Hospital, University of Antwerp, Antwerp, Belgium [37]Department of Neuropediatrics, Christian-Albrechts-University of Kiel, Germany. [38]Division of Neurology, Children's Hospital of Philadelphia, Philadelphia, USA [39]Department of Neuropediatrics, University of Tübingen, Tübingen, Germany. [40]Department of Diagnostics, Institute of Human Genetics, University of Leipzig, Leipzig, Germany.

[#] These authors contributed equally to this work.

Abstract

Epileptic encephalopathies are a phenotypically and genetically heterogeneous group of severe epilepsies accompanied by intellectual disability and other neurodevelopmental features[1-6]. Using next generation sequencing, we identified four different *de novo* mutations in *KCNA2*, encoding the potassium channel $K_V1.2$, in six patients with epileptic encephalopathy (one mutation recurred three times independently). Four individuals presented with febrile and multiple afebrile, often focal seizure types, multifocal epileptiform discharges strongly activated by sleep, mild-moderate intellectual disability, delayed speech development and sometimes ataxia. Functional studies of the two mutations associated with this phenotype revealed an almost complete loss-of-function with a dominant-negative effect. Two further individuals presented with a different and more severe epileptic encephalopathy phenotype. They carried mutations inducing a drastic gain-of-function effect leading to permanently open channels. These results establish *KCNA2* as a novel

gene involved in human neurodevelopmental disorders by two different mechanisms, predicting either hyperexcitability or electrical silencing of K_V1.2-expressing neurons.

Many of the voltage-gated potassium channels (K_V1–12) are expressed in the central nervous system (CNS), playing an important role in neuronal excitability and neurotransmitter release[7]. Mutations in potassium channel-encoding genes cause different neurological diseases, including benign familial neonatal seizures (*KCNQ2*/K_V7.2, *KCNQ3*/K_V7.3)[8-10], neonatal epileptic encephalopathy (*KCNQ2*)[11,12], episodic ataxia type 1 (EA1) (*KCNA1*/K_V1.1)[13], and peripheral nerve hyperexcitability (*KCNA1*, *KCNQ2*)[13-15]. In addition, antibodies against K_V1.1 or associated proteins like Contactin-associated protein 2 (Caspr2) or Leucine-rich, glioma-inactivated 1 protein (LGI1) cause limbic encephalitis or neuromyotonia[16]. Therefore, potassium channel genes represent interesting candidates for neurodevelopmental disorders.

To identify mutations in presumed genetic forms of epilepsy, we designed a targeted re-sequencing panel[17] comprising 265 known and 220 candidate genes for epilepsy (Supplementary Table 1). Screening a pilot cohort of 33 patients, we identified mutations in known epilepsy genes in 16 cases[17]. The remaining 17 cases were evaluated for mutations in candidate genes (Supplementary note), which led to the detection of a heterozygous *de novo* mutation in *KCNA2*, c.1214C>T, p.Pro405Leu (P405L), affecting the highly-conserved pore domain of the voltage-gated potassium channel K_V1.2. This mutation is not found in control databases (1000G, EVS, dbSNP138, ExAC).

The female Patient #1 carrying this mutation had unremarkable early development until epilepsy onset at 17 months old. The phenotype included febrile and afebrile alternating hemiclonic seizures and status epilepticus, reminiscent of Dravet syndrome. The electroencephalogram (EEG) showed multifocal spikes with marked activation during sleep. After seizure onset, ataxia and delay of psychomotor and language development became apparent. She had postnatal short stature, growth hormone deficiency and hypothyroidism. Seizures and ataxia responded poorly to antiepileptic drugs (topiramate, oxcarbazepine, valproic acid, bromide), including acetazolamide (known to be effective in EA1 caused by mutations in *KCNA1*[18]). At last follow-up at eight years old, she had remained seizure-free for the past six months without previous change of medication.

Further *KCNA2* mutations were identified in several parallel studies (Supplementary Fig. 1). First, we performed whole exome sequencing (WES) in 86 parent-offspring trios with epileptic encephalopathy (31 with *SCN1A*-negative Dravet syndrome [DS], 39 with myoclonic-atonic epilepsy [MAE], and 16 with electrical status epilepticus in slow-wave sleep [ESES]). Second, we performed panel sequencing (Supplemental note) in 147 adult patients with a broad spectrum of epilepsy phenotypes associated with intellectual disability. Third, we performed WES in an adult cohort of 10 independent trios with severe epilepsy and intellectual disability, and WES in another cohort of 12 independent, isolated index cases with early-onset ataxia and epilepsy. We identified six additional independent cases with previously-unreported heterozygous *KCNA2* variants (Table 1, Supplementary note): Patient #2 (initially classified as MAE) carried the *de novo* mutation c.788T>C, p.Ile263Thr (I263T). Patient #3 (intellectual disability with neonatal-onset focal epilepsy and cerebellar

Europe PMC Funders Author Manuscripts

hypoplasia) carried the variant c.440G>A, p.Arg147Lys (R147K), of unknown inheritance. Since (i) it could not be confirmed as *de novo*, (ii) was predicted as benign from seven out of nine prediction tools, (iii) lysine occurs naturally at that position in drosophila and zebrafish, and (iv) did not reveal functional consequences, R147K was considered a variant of unknown significance (see Supplementary note, Supplementary Tables 1 and 2, and Supplementary Fig. 3). Patients #4 (initially classified as DS with prominent focal seizures) and #5 (intellectual disability with febrile seizures, focal seizures and status epilepticus) also carried the *de novo* P405L mutation (Fig. 1c and Supplementary Fig. 2). Patients #1, #2, #4 and #5 eventually became seizure-free between four and 15 years old, whereas intellectual disability and (in #1 and #4) mild to moderate ataxia remained unchanged. Recurrence of P405L in three independent cases suggests a mutational hotspot: c.1214 is located in a stretch of cytosines and guanines and the C>T mutation likely occurs due to a methylated CpG sequence, possibly bypassing the DNA repair system and so becoming prone to this pyrimidine-pyrimidine substitution.

Patient #6 carried the *de novo* mutation c.894G>T, p.Leu298Phe (L298F). His phenotype was different and much more severe, presenting with severe intellectual disability with gradual loss of language and motor skills, pharmacoresistant generalized tonic-clonic, atypical absence and myoclonic seizures, facial dysmorphism, generalized epileptic discharges and moderate ataxia (Table 1 and Supplementary note). Similarly, patient #7 carrying the *de novo* mutation c.890G>A, p.Arg297Gln (R297Q) presented with a more severe phenotype consisting of moderate intellectual disability, moderate to severe ataxia and pharmacoresistant seizures.

We subsequently screened a follow-up cohort of 99 patients, comprising 47 individuals with unresolved epileptic encephalopathy, short stature and/or ataxia as well as 52 individuals with intellectual disability and idiopathic severe GH deficiency without detecting additional sequence alterations by Sanger sequencing. We excluded copy number variations affecting *KCNA2* in all 99 follow-up cases as well as 86 trio-WES cases using an in-house-developed multiplex amplicon quantification technique (Online Methods and Supplementary Fig. 1).

To validate our findings statistically and corroborate *KCNA2* as a new disease-predisposing gene for epileptic encephalopathy, we calculated the probability for recurring *KCNA2* mutations occurring by chance in our cohorts. Comparing the allele frequency of six (two times P405L) *KCNA2* non-synonymous variants in our validation cohorts (6/(354×2), excluding the first P405L mutation detected in the discovery cohort of 33 patients) with those missense and nonsense variants reported in the largest available control database (ExAC, 144/122828), revealed a significant enrichment of *KCNA2* variants in our patient cohorts using Fisher's exact test ($p=2.6\times10^{-4}$). Further statistical evidence is provided in the Supplementary Note. *KCNA2* had not been associated with a human disease so far. However, during the review process of this manuscript, a single case report was published describing a 7-year-old boy with the *KCNA2 de novo* mutation R297Q presenting with ataxia and myoclonic epilepsy, similar to our patient #7.[19] In addition, the *Pingu* mouse presenting with ataxia and growth retardation carries a *Kcna2* loss-of-function mutation, p.Ile402Thr, in close proximity to P405L; *Kcna2* knock-out mice present with severe seizures and premature death[20,21].

$K_V1.2$ belongs to the K_V1 family ($K_V1.1$–8), all members of which are expressed in the CNS. These channels consist of four subunits with six transmembrane segments (S1-S6). S4 forms the voltage-sensor and S5-S6 the pore region containing a selectivity filter and gating ion flow[22] (Fig. 1a). All four *KCNA2* sequence alterations detected in patients #1–7 (except the one in #3) are localized in highly-conserved and functionally-important protein regions (Fig. 1b), and were predicted as pathogenic. P405L disrupts the highly-conserved, K_V-specific PVP motif in S6, which is thought to link the gate to the voltage-sensor[23,24]. A PVP>AVP mutation in $K_V1.5$ leads to a non-functional channel[25]. I263T in S3 may disrupt a hydrophobic segment proposed to focus the electric field across the cell membrane, thus enabling the S4 gating charges to translocate over a smaller distance rather than the entire depth of the membrane bilayer[26]. Furthermore, I263T in $K_V1.2$ corresponds to I262T in $K_V1.1$ causing EA1 with distal weakness.[27] Finally, R297Q and L298F directly affect the S4 voltage sensor, and R297Q has been described before to induce a negative shift of the activation curve.[27,28]

Functional effects of all detected sequence alterations were examined using an automated two-microelectrode voltage-clamp oocyte testing system. We found a sigmoidal relationship between the amount of injected wildtype (WT) cRNA and potassium current amplitude, with a strong decrease in amplitude for the 8-fold cRNA amount (Fig. 2b, Supplementary Fig. 5). This quantitative titration of protein levels by varying the amounts of injected RNA was used to determine the amount of injected cRNA for further experiments. For P405L and I263T, we found a dramatic reduction of current amplitudes and thus a clear loss of channel function (Figs. 2c). When either of the two mutations were co-expressed with WT $K_V1.2$ in a 1:1, 1:2 or 1:4 ratio, with constant amount of injected WT cRNA, current amplitudes significantly decreased (Figs. 2d) compared with similar amounts of WT alone (Fig. 2b). Hence, both P405L and I263T exert a clear dominant-negative effect on WT $K_V1.2$ channels. Furthermore, I263T caused a depolarizing shift of voltage-dependent activation, and slight changes in inactivation were found for P405L (Supplementary Fig. 4).

In contrast to P405L and I263T, both R297Q and L298F induced strong gain-of-function effects. Neutralization of the second arginine in the voltage sensor in $K_V1.2$-R297Q increased current amplitudes by 9-fold and shifted the voltage dependence of steady-state activation by –40 mV compared with WT (Fig. 3a–c), The gain-of-function of the L298F mutation was even more pronounced with a 13-fold increase in current amplitudes and a –50 mV shift of the activation curve (Fig. 3a–c). As a consequence of the permanently open mutant channels, resting membrane potentials of oocytes expressing R297Q or L298F channels were about 40 mV more negative than of those expressing WT (Fig. 3d). Both mutations exerted a dominant effect on the WT, since co-injection of either R297Q or L298F with WT in a 0.5:0.5 ratio revealed very similar alterations as with one of the mutations (1.0) alone (Fig. 3b–d).

To examine protein production and stability, we performed SDS-page analysis of total cell lysates using a monoclonal anti-$K_V1.2$ antibody. Representative Western blots show that all mutations generate a protein expression level similar to the 57-kD band of the WT (Figs. 2e and 3e). A slight but reproducible shift was found for the band of P405L in both oocytes and mammalian cells (Fig. 2e, top, middle). Steric properties of proline can disrupt secondary

structure elements, which could be important for the function of the conserved PVP motif. A leucine in this position (LVP) could induce a structural change resulting in altered gel migration[28].

K_V1.2 belongs to the delayed rectifier class of potassium channels enabling efficient neuronal repolarization following an action potential. Loss-of-function mutations predict hyperexcitable neuronal membranes and repetitive neuronal firing due to impaired repolarization. This hypothesis is corroborated by the epileptic phenotype of the *Kcna2* knock-out mouse[21]. In stark contrast, R297Q and L298F predict permanently open channels at physiological membrane potentials, and electrical silencing by membrane hyperpolarization (as observed in oocytes). It is difficult to speculate about the pathophysiological consequences of a K_V1.2 loss- or gain-of-function beyond the level of single neurons, particularly since this channel has been detected in a broad range of both excitatory and inhibitory neurons[29,30]. Further experiments in gene-targeted mouse models could answer these questions.

In summary, we identified *de novo* mutations in *KCNA2* causing mild to severe epileptic encephalopathy in roughly 1.7% of cases across our different cohorts. The phenotype associated with dominant-negative loss-of-function mutations comprised infantile/early-childhood seizure onset, frequent febrile and afebrile focal motor and dyscognitive seizures with overlap to DS (#1, #4, #5) and MAE (#2). However, focal seizures are uncommon in these syndromes and in particular the observed multifocal epileptiform discharges with marked activation during sleep are not described either in DS or MAE. All four patients became seizure-free between four and 15 years old with no apparent association to a recent change of medication. Thus, this improvement might either be due to a cumulative treatment response or simply represent a spontaneous resolution (Table 1, Supplementary note). Initially normal psychomotor development slowed after seizure onset, resulting in mild-moderate intellectual disability associated with mild-moderate ataxia and continuous myoclonus in some cases. By contrast, the phenotypes of patients #6 and #7, carrying mutations with dominant gain-of-function, were more severe in terms of epilepsy, ataxia and intellectual disability, and also differed electrographically, with generalized epileptic discharges. This may suggest that different pathomechanisms underlie distinctive clinical symptoms. Clinical-genetic studies and correlation with functional investigations from additional patients with further mutations are needed to confirm this genotype-phenotype relationship.

Online Methods

Whole exome and panel sequencing analysis

High throughput sequencing has been performed as described previously by our group for whole exome analysis[31] and panel analysis[17].

The panel used to screen the pilot cohort of 33 patients (including the index patient) comprised 485 known and putative epilepsy genes. (Supplementary Table 1) The candidates comprised genes that were suggestive for being involved in epileptogenesis due to several reasons, e.g. genes belong to neurotransmitter receptor families or other ion channels, genes

were discussed by different research groups as putatively involved in epilepsy, genes are associated with seizures in animals or associated with human neurodevelopmental phenotypes, etc. The gene panel used to screen the second cohort of 147 patients was an updated version of the initial panel. To improve sequence coverage and adapting the panel for purely diagnostic purposes, we excluded a few metabolic and mitochondrial genes as well as most candidate genes and added all recently published novel epileptic encephalopathy genes. This panel finally contained 280 genes including 20 candidates for research settings (Supplementary Table 2).

Sanger sequencing analysis and CNV analysis

We performed bidirectional Sanger sequencing of all three exons of *KCNA2* (ENST00000485317, NM_004974) and its intron-exon boundaries using the BigDye Terminator v3.1 Cycle Sequencing kit on an ABI3730XL DNA Analyzer (Applied Biosystems, Foster City, CA; primers available upon request) in 47 patients with epileptic encephalopathy and ataxia and/or short stature as well as 52 patients with intellectual disability and severe growth hormone deficiency.

Additionally, the genomic region containing *KCNA2* was screened for CNVs by use of an in-house-developed technique for multiplex amplicon quantification (MAQ). With this MAQ technique, we screened all 99 individuals of the Sanger sequencing cohort as well as all 86 individuals of the WES cohort (Supplementary Fig. 1). This assay comprises a multiplex PCR amplification of fluorescently-labeled target and reference amplicons, followed by fragment analysis on the ABI3730 DNA Analyzer[32]. The comparison of normalized peak areas between the test individual and the average of seven control individuals results in the target amplicon doses indicating the copy number of the target amplicon (using the in-house developed Multiplex Amplicon Quantification Software. The multiplex PCR reaction consists of three test amplicons located in the genomic region of *KCNA2* and three reference amplicons located on different chromosomes (primer mix is available upon request).

Pathogenicity prediction—For the prediction of the pathogenicity of nonsynonymous variants we used the ANNOVAR[33] table_annovar.pl script together with the LJB23 database (dbNSFP)[34] from June 2013 comprising prediction scores from SIFT, Polyphen2 (HDIV and HVAR), LRT, MutationTaster, MutationAssessor, FATHMM, MetaSVM and MetaLR scores. Scores were used as given on the ANNOVAR webpage. Additional three conservation scores (GERP+, PhyloP, SiPhy) were used to determine the conservation of a genomic position (More details in Supplementary Table 2).

Testing the enrichment of pathogenic variants—To test the enrichment of probably damaging nonsynonymous *KCNA2* variants in our data, we used the Exome Aggregation Consortium (ExAC) database as a control dataset. It comprises data from 61,486 individuals coming from various exome sequencing projects including control cohorts data but also data from studies on neurological disorders like schizophrenia and bipolar disorder. We extracted all 64 nonsynonymous (missense and nonsense) variants for *KCNA2* from ExAC [11/2014]. Some of them occurred in more than one individual yielding altogether 144 alleles with

variation in *KCNA2* out of a total number of 122828 alleles in the ExAC database. Significant enrichment of nonsynonymous variants was then tested determining the difference of allele counts in our data and the ExAC dataset using Fisher's exact test.

Probability assessment of *de novo* mutation events

We first obtained an estimate for the single-nucleotide mutation rate in the *KCNA2* gene. This rate equals the product of the average *de novo* mutation rate in humans of 1.2×10^{-8} per nucleotide per generation[35] and the length of the largest coding sequence of *KCNA2* (coding ID in CCDS database: 827.1) of 1,500 base pairs, yielding 1.8×10^{-5} per generation. The probability of observing a *de novo* mutation in *KCNA2* in *k* out of *n* parent-offspring trios then simply follows a binomial distribution with a success probability equaling the gene-based mutation rate, $\mathrm{Bin}(n, k, 1.8\times10^{-5})$.

Functional investigations

Mutagenesis and RNA preparation—Site-directed mutagenesis was performed to engineer the mutations into the human *KCNA2* cDNA using Quickchange™ (Agilent Technologies, USA; primers are available upon request). The mutant cDNA was fully resequenced before being used in experiments to confirm the introduced mutation and exclude any additional sequence alterations. cRNA was prepared using the SP6 mMessage kit from Ambion. The human $K_V1.2$ in the pcDNA3.1 vector was kindly provided by Stephan Grissmer (Institute of Applied Physiology, Ulm University).

Electrophysiology—*Xenopus laevis* oocytes were obtained from the Institute of Physiology I, Tübingen. Preparation of the oocytes was performed as described previously[12]. Oocytes were treated with collagenase (1 mg/ml of type CLS II collagenase, Biochrom KG) in OR-2 solution (in mM: 82.5 NaCl, 2.5 KCl, 1 $MgCl_2$ and 5 Hepes, pH 7.5) followed by three washing steps and storage at 16°C in Barth solution (in mM: 88 NaCl, 2.4 $NaHCO_3$, 1 KCl, 0.33 $Ca(NO_3)_2$, 0.41 $CaCl_2$, 0.82 $MgSO_4$ and 5 Tris/HCl, pH 7.4 with NaOH) supplemented with 50 μg/ml gentamicin (Biochrm KG). 50 nl of cRNA encoding wildtype (WT) or mutated $K_V1.2$ subunits (1μg/μl) was injected into oocytes using the Roboocyte2 (Multi Channel Systems, Reutlingen, Germany) and stored for two days (at 17°C) prior to the experiment. Amplitudes of currents of WT and mutant channels recorded on the same day were normalized to the mean value of the 1.0 $K_V1.2$ WT on that day to pool the normalized data from different experiments together.

Automated two-electrode voltage-clamp—Potassium currents in oocytes were recorded at room temperature (20-22°C) using Roboocyte2 (Multi channel Systems, Reutlingen, Germany). For two-electrode voltage-clamp (TEVC) recordings, oocytes were impaled with two glass electrodes with a resistance of 0.4 – 1 MΩ containing 1 M KCl/ 1.5 M KAc and clamped at a holding potential of −80 mV. Oocytes were perfused with a ND96 bath solution containing (in mM): 93.5 NaCl, 2 KCl, 1.8 $CaCl_2$, 2 $MgCl_2$, 5 HEPES (pH 7.6). Currents were sampled at 5 kHz.

Voltage clamp protocols and data analysis—The membrane was depolarized to various test potentials from a holding potential of −80 mV to record potassium currents. The

activation curve (conductance–voltage relationship) was derived from the current–voltage relationship that was obtained by measuring the peak current at various step depolarizations from the holding potential of –80 mV (10 mV increment, depolarized to +70 mV). The following Boltzmann function was fitted to the obtained data points:

$$g(V) = \frac{g_{max}}{\left\{1+\exp\left[\left(V - V_{1/2}\right)/k_v\right]\right\}}$$

with g (V) = I/(V-V_{rev}) being the conductance, I the recorded current amplitude at test potential V, V_{rev} the potassium reversal potential, g_{max} the maximal conductance, $V_{1/2}$ the voltage of half-maximal activation and k_V a slope factor. Voltage-dependent inactivation of WT and mutated K_V1.2 channels were analyzed using 25-s conditioning pulses at potentials ranging –60 mV to 0 mV (increment 10 mV) from a holding of –80 mV, the test pulse was 30 mV. A standard Boltzmann function was fitted to the inactivation curves:

$$I(V) = \frac{I_{max}}{\left\{1+\exp\left[\left(V - V_{1/2}\right)/k_v\right]\right\}}$$

with I being the recorded current amplitude at the conditioning potential V, I_{max} being the maximal current amplitude, $V_{1/2}$ the voltage of half-maximal inactivation, and k_V a slope factor.

Western Blot Analysis—For Western blot, injected *Xenopus* oocytes were lysed in a buffer containing (in mM) 20 Tris, 100 NaCl, 1 ethylenediaminetetraacid, 0.5% Triton X-100 and 10% glycerol with protease inhibitor cOmplete (Roche, Basel, Switzerland). In addition, for the P405L mutation CHO cells were transfected with 10 *μ*g/*μ*l DNA using Mirus "TransIT®-LT1" reagent. CHO cells were lysed in a buffer containing (in M): 2 Tris (pH 7.5), 3 NaCl, 0.2 EDTA, 0.2 EGTA, 0.25 Napyrophosphate, 0.1 β-glycerolphosphate, 0.1 sodium-orthovanadate, 1 DTT, 0.1 1% Triton and 25x cOmplete solution (Roche). For measuring protein concentrations (BCA systems, Thermo Fisher Scientific) 15 – 20 *μ*g of protein was separated by sodium dodecyl sulfate-polyacrylamide gel electrophoresis (SDS Page) on 8% polyacrylamide gels. The proteins were transferred onto polyvinylidene fluoride (PVDF) membranes (PALL Corporation, Port Washington, NY), and Western blotting was performed using a mouse-Anti-K_V1.2 antibody (NeuroMab clone K14/16). Water-injected oocytes, untransfected (u.t.) and water transfected (Mock) CHO cells were used as controls.

Data and statistical analysis—Sample size was estimated by using GraphPad StatMate Software. TEVC recordings were analyzed using Roboocyte 2+ (Multi Channel Systems, Germany) and Clampfit (pClamp, Axon Instruments), Origin 6.1 (Origin-Lab Corp., Northampton, USA), and Excel (Microsoft, USA) software. Data were tested for normal distribution using SigmaPlot12 (Systat Software). For statistical evaluation one-way ANOVA with Dunnett's posthoc test (normally distributed data) or one-way ANOVA on ranks with Dunn's posthoc test (not-normally distributed data) was used for comparing

multiple groups, with one-way ANOVA testing the overall difference between groups and posthoc tests telling the difference between specific groups. For unpaired data sets Student's t-test (normally distributed unpaired data sets) or Mann-Whitney rank-sum (not-normally distributed) were used. All data are shown as mean ± SEM. For all statistical tests, significance with respect to control is indicated in the figures using the following symbols: *p<0.05, **p<0.01, ***p<0.001.

Supplementary Material

Refer to Web version on PubMed Central for supplementary material.

Acknowledgements

We thank all patients and family members for their participation in this study, Dr. S. Grissmer for providing the human cDNA clone of *KCNA2*, and Dr. F. Lang and his colleagues from the Institute of Physiology I, University of Tuebingen, for providing *Xenopus laevis* oocytes. J.R.L. (32EP30_136042 / 1), J.M.S. (EUI-EURC2011-4325), H.Le. (DFG Le1030/11-1), P.D.J. (G.A.136.11.N, FWO/ESF-ECRP), and I.H. (DFG HE 5415 3-1) received financial support within the EuroEPINOMICS-RES and - CoGIE networks (www.euroepinomics.org), a Eurocores project of the European Science Foundation. R.S. received funding from the European Union (E-Rare JTC grant 01GM1408B and PIOF-GA-2012-326681). J.M.S. received further support from the Ministerio de Economía y Competitividad (SAF2010-18586). H.Le., S.B., and S.Ma. received further support from the Federal Ministry for Education and Research (BMBF, program on rare diseases, IonNeurONet: 01GM1105A). S.Z. received support from the NIH (R01NS072248). S.M.S. received support from the Wellcome Trust (084730), NIHR UCLH Biomedical Research Centre and Epilepsy Society, UK. M.Sy. received support by the Interdisciplinary Center for Clinical Research IZKF Tübingen (2191-0-0). A.S. received funding for a postdoctoral fellowship by the Fonds Wetenschappelijk Onderzoek. T.D. is a PhD fellow of the Institute of Science and Technology (IWT).

EuroEPINOMICS RES Consortium:

Rudi Balling[19], Nina Barisic[43], Stéphanie Baulac[44-46], Hande S Caglayan[14], Dana C. Craiu[26,27], Peter De Jonghe[6,7,36], Christel Depienne[44,46,47], Padhraig Gormley[34], Renzo Guerrini[48], Ingo Helbig[37,38], Helle Hjalgrim[8], Dorota Hoffman-Zacharska[28], Johanna Jähn[37], Karl Martin Klein[49], Bobby P.C. Koeleman[50], Vladimir Komarek[25], Roland Krause[19], Eric LeGuern[44-46,51], Anna-Elina Lehesjoki[22,23,24], Johannes R. Lemke[1,4,40], Holger Lerche[2], Carla Marini[48], Patrick May[19], Rikke S. Møller[8,9], Hiltrud Muhle[37], Aarno Palotie[33,34,35], Deb Pal[52], Felix Rosenow[49], Kaja Selmer[53,54], José M. Serratosa[16,17], Sanjay M. Sisodiya[10,11], Ulrich Stephani[37], Katalin Sterbova[25], Pasquale Striano[55], Arvid Suls[6,7], Tiina Talvik[56,57], Sarah von Spiczak[37], Yvonne Weber[2], Sarah Weckhuysen[6,7] & Federico Zara[58]

[43]Department of Paediatrics, University of Zagreb, Medical School, University Hospital Centre Zagreb, Zagreb, Croatia.

[44]INSERM UMR 975, Institut du Cerveau et de la Moelle Epinière, Hôpital Pitié-Salpêtrière, Paris, France.

[45]CNRS 7225, Hôpital Pitié-Salpêtrière, Paris, France.

[46]Université Pierre et Marie Curie–Paris 6 (UPMC), UMRS 975, Paris, France.

[47]Institüt für Humangenetik, Universität Würzburg, Würzburg, Germany.

Europe PMC Funders Author Manuscripts

[48]Pediatric Neurology Unit and Laboratories, Children's Hospital A. Meyer, University of Florence, Florence, Italy.

[49]Epilepsy Center Hessen, Department of Neurology, University Hospitals Marburg and Philipps, University Marburg, Marburg, Germany.

[50]Department of Medical Genetics, University Medical Center Utrecht, Utrecht, The Netherlands.

[51]Assistance Publique–Hôpitaux de Paris (AP-HP), Hôpital Pitié-Salpêtrière, Département de Génétique et de Cytogénétique, Unité Fonctionnelle de Neurogénétique Moléculaire et Cellulaire, Paris, France.

[52]Department of Clinical Neuroscience, Institute of Psychiatry, King's College London, London, UK.

[53]Department of Medical Genetics, Oslo University Hospital, Oslo, Norway.

[54]Institute of Medical Genetics, University of Oslo, Oslo, Norway.

[55]Pediatric Neurology and Muscular Diseases Unit, Department of Neurosciences, Rehabilitation, Ophthalmology, Genetics, Maternal and Child Health, 'G Gaslini Institute', Genova, Italy.

[56]Department of Pediatrics, University of Tartu, Tartu, Estonia.

[57]Department of Neurology and Neurorehabilitation, Children's Clinic, Tartu University Hospital, Tartu, Estonia.

[58]Laboratory of Neurogenetics, Department of Neurosciences, Gaslini Institute, Genova, Italy.

URLs.

dbSNP Build 138, http://www.ncbi.nlm.nih.gov/projects/SNP/; 1000 Genomes Project database, http://www.1000genomes.org/; Exome Variant Server, http://evs.gs.washington.edu/EVS/; ExAC, http://exac.broadinstitute.org/; PolyPhen-2, http://genetics.bwh.harvard.edu/pph2/; MutationTaster, http://www.mutationtaster.org/; Multiplex Amplicon Quantification, http://www.multiplicom.com/multiplex-amplicon-quantification-maq; Multiplex Amplicon Quantification Software, http://www.multiplicom.com/maq-s; ANNOVAR, http://www.openbioinformatics.org/annovar/annovar_filter.html#ljb23; GEM.app browser, https://genomics.med.miami.edu/.

References

1. Capovilla G, Wolf P, Beccaria F, Avanzini G. The history of the concept of epileptic encephalopathy. Epilepsia. 2013; 54(Suppl 8):2–5.
2. Guerrini R, Pellock JM. Age-related epileptic encephalopathies. Handb Clin Neurol. 2012; 107:179–93. [PubMed: 22938971]

3. Claes L, et al. *De novo* mutations in the sodium-channel gene *SCN1A* cause severe myoclonic epilepsy of infancy. Am J Hum Genet. 2001; 68:1327–32. [PubMed: 11359211]
4. Nava C, et al. De novo mutations in *HCN1* cause early infantile epileptic encephalopathy. Nat Genet. 2014; 46:640–5. [PubMed: 24747641]
5. Epi KC, et al. De novo mutations in epileptic encephalopathies. Nature. 2013; 501:217–21. [PubMed: 23934111]
6. Lerche H, et al. Ion channels in genetic and acquired forms of epilepsy. J Physiol. 2013; 591:753–64. [PubMed: 23090947]
7. Lai HC, Jan LY. The distribution and targeting of neuronal voltage-gated ion channels. Nature Reviews Neuroscience. 2006; 7:548–562. [PubMed: 16791144]
8. Biervert C, et al. A potassium channel mutation in neonatal human epilepsy. Science. 1998; 279:403–6. [PubMed: 9430594]
9. Charlier C, et al. A pore mutation in a novel KQT-like potassium channel gene in an idiopathic epilepsy family. Nat Genet. 1998; 18:53–5. [PubMed: 9425900]
10. Singh NA, et al. A novel potassium channel gene, KCNQ2, is mutated in an inherited epilepsy of newborns. Nat Genet. 1998; 18:25–9. [PubMed: 9425895]
11. Weckhuysen S, et al. *KCNQ2* encephalopathy: emerging phenotype of a neonatal epileptic encephalopathy. Ann Neurol. 2012; 71:15–25. [PubMed: 22275249]
12. Orhan G, et al. Dominant-negative effects of *KCNQ2* mutations are associated with epileptic encephalopathy. Ann Neurol. 2014; 75:382–94. [PubMed: 24318194]
13. Browne DL, et al. Episodic ataxia/myokymia syndrome is associated with point mutations in the human potassium channel gene, *KCNA1*. Nat Genet. 1994; 8:136–40. [PubMed: 7842011]
14. Wuttke TV, et al. Peripheral nerve hyperexcitability due to dominant-negative *KCNQ2* mutations. Neurology. 2007; 69:2045–53. [PubMed: 17872363]
15. Dedek K, et al. Myokymia and neonatal epilepsy caused by a mutation in the voltage sensor of the KCNQ2 K+ channel. Proc Natl Acad Sci U S A. 2001; 98:12272–7. [PubMed: 11572947]
16. Irani SR, et al. Antibodies to K_V1 potassium channel-complex proteins leucine-rich, glioma inactivated 1 protein and contactin-associated protein-2 in limbic encephalitis, Morvan's syndrome and acquired neuromyotonia. Brain. 2010; 133:2734–48. [PubMed: 20663977]
17. Lemke JR, et al. Targeted next generation sequencing as a diagnostic tool in epileptic disorders. Epilepsia. 2012; 53:1387–98. [PubMed: 22612257]
18. Lubbers WJ, et al. Hereditary myokymia and paroxysmal ataxia linked to chromosome 12 is responsive to acetazolamide. J Neurol Neurosurg Psychiatry. 1995; 59:400–5. [PubMed: 7561920]
19. Pena SD, Coimbra RL. Ataxia and myoclonic epilepsy due to a heterozygous new mutation in KCNA2: proposal for a new channelopathy. Clin Genet. 2015; 87:e1–3. [PubMed: 25477152]
20. Xie G, et al. A new $K_V1.2$ channelopathy underlying cerebellar ataxia. J Biol Chem. 2010; 285:32160–73. [PubMed: 20696761]
21. Brew HM, et al. Seizures and reduced life span in mice lacking the potassium channel subunit $K_V1.2$, but hypoexcitability and enlarged K_V1 currents in auditory neurons. J Neurophysiol. 2007; 98:1501–25. [PubMed: 17634333]
22. Jan LY, Jan YN. Voltage-gated potassium channels and the diversity of electrical signalling. J Physiol. 2012; 590:2591–9. [PubMed: 22431339]
23. Holmgren M, Shin KS, Yellen G. The activation gate of a voltage-gated K^+ channel can be trapped in the open state by an intersubunit metal bridge. Neuron. 1998; 21:617–21. [PubMed: 9768847]
24. Long SB, Campbell EB, Mackinnon R. Voltage sensor of $K_V1.2$: structural basis of electromechanical coupling. Science. 2005; 309:903–8. [PubMed: 16002579]
25. Labro AJ, Raes AL, Bellens I, Ottschytsch N, Snyders DJ. Gating of shaker-type channels requires the flexibility of S6 caused by prolines. J Biol Chem. 2003; 278:50724–31. [PubMed: 13679372]
26. Chen X, Wang Q, Ni F, Ma J. Structure of the full-length Shaker potassium channel $K_V1.2$ by normal-mode-based X-ray crystallographic refinement. Proc Natl Acad Sci U S A. 2010; 107:11352–7. [PubMed: 20534430]

27. Klein A, Boltshauser E, Jen J, Baloh RW. Episodic ataxia type 1 with distal weakness: a novel manifestation of a potassium channelopathy. Neuropediatrics. 2004; 35:147–9. [PubMed: 15127317]

28. Nybo K. Molecular biology techniques Q&A. Western blot: protein migration. Biotechniques. 2012; 53:23–4. [PubMed: 22780315]

29. Lorincz A, Nusser Z. Cell-type-dependent molecular composition of the axon initial segment. J Neurosci. 2008; 28:14329–40. [PubMed: 19118165]

30. Wang H, Kunkel DD, Schwartzkroin PA, Tempel BL. Localization of Kv1.1 and Kv1.2, two K channel proteins, to synaptic terminals, somata, and dendrites in the mouse brain. J Neurosci. 1994; 14:4588–99. [PubMed: 8046438]

31. Suls A, et al. De novo loss-of-function mutations in CHD2 cause a fever-sensitive myoclonic epileptic encephalopathy sharing features with Dravet syndrome. Am J Hum Genet. 2013; 93:967–75. [PubMed: 24207121]

32. Suls A, et al. Microdeletions involving the SCN1A gene may be common in SCN1A-mutation-negative SMEI patients. Hum Mutat. 2006; 27:914–20. [PubMed: 16865694]

33. Wang H, Kunkel DD, Martin TM, Schwartzkroin PA, Tempel BL. Heteromultimeric K^+ channels in terminal and juxtaparanodal regions of neurons. Nature. 1993; 365:75–9. [PubMed: 8361541]

34. Liu X, Jian X, Boerwinkle E. dbNSFP v2.0: a database of human non-synonymous SNVs and their functional predictions and annotations. Hum Mutat. 2013; 34:E2393–402. [PubMed: 23843252]

35. Kong A, et al. Rate of *de novo* mutations and the importance of father's age to disease risk. Nature. 2012; 488:471–5. [PubMed: 22914163]

Europe PMC Funders Author Manuscripts

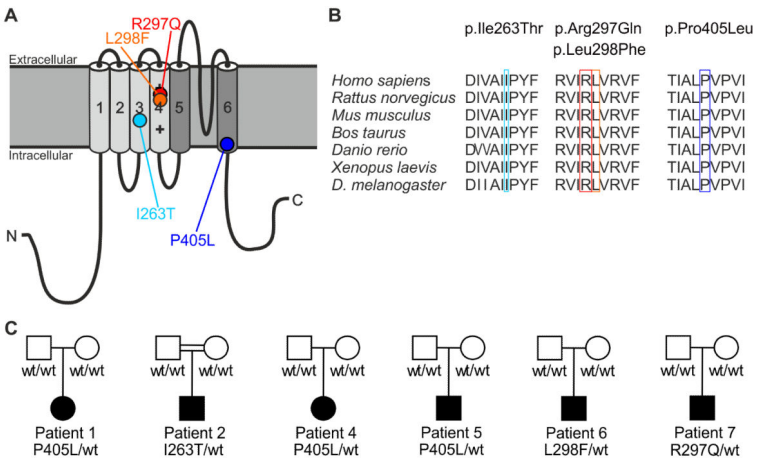

Figure 1.

Mutations in the $K_V1.2$ channel. **(A)** Structure of the voltage-gated potassium channel $K_V1.2$ with transmembrane segments S1–S4 forming the voltage sensor domain (light gray) and the pore region S5-S6 (in dark gray) with its pore-forming loop. Mutations are localized in highly-conserved regions in the S3 segment (I263T, light blue), the S4 segment constituting the voltage sensor (R297Q, red; L298F, orange) and the S6 segment (P405L, dark blue). **(B)** I263, R297, L298 and P405 and the respective surrounding amino acids show evolutionary conservation. **(C)** Pedigrees of patients #1, #2 and #4–7.

Europe PMC Funders Author Manuscripts

Europe PMC Funders Author Manuscripts

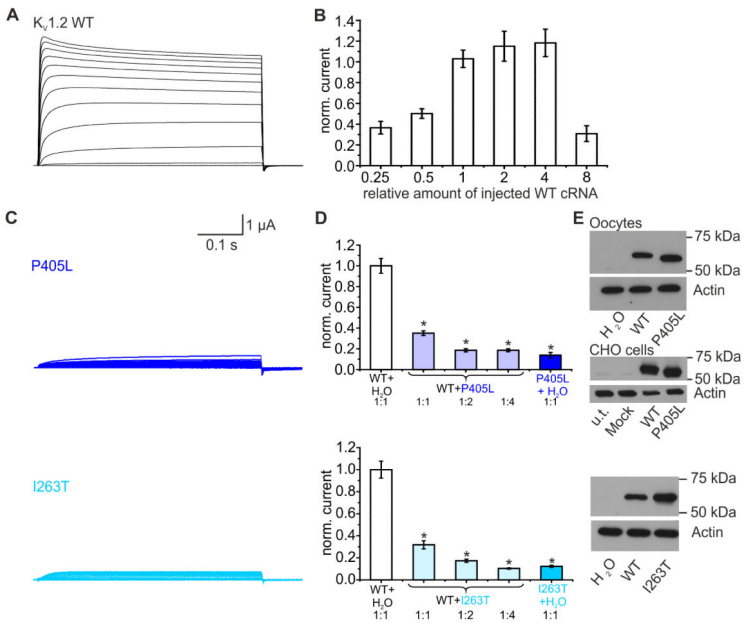

Figure 2.

Functional effects of the *KCNA2* mutations P405L and I263T. **(A)** Representative current traces of $K_V1.2$ wildtype (WT) channels recorded in a *Xenopus laevis* oocyte during voltage steps (from −80 mV to +70 mV). **(B)** Effect of increasing amounts of injected WT-*KCNA2* cRNA on current amplitude (0.25: n=13; 0.5: n=18; 1: n=22; 2: n=17; 4: n=20; 8: n=19). Shown are means ± SEM. **(C)** Current traces derived from $K_V1.2$-P405L (top) and $K_V1.2$-I263T (bottom) channels recorded as described in (A). **(D)** K^+-currents were reduced for mutants P405L (top) and I263T (bottom) compared to WT-cRNA (top: P405L: n=10; WT: n=44; bottom: I263T: n=10; WT: n=34). A dominant-negative effect of P405L and I263T mutants on $K_V1.2$-WT channels was shown when a constant amount of WT cRNA (amount 1 in (B)) was injected with either H_2O or increasing amounts of mutant cRNA (top: P405L: ratio 1:1: n=47; ratio 1:2: n=40; ratio 1:4: n=36; bottom: I263T: ratio 1:1: n=34; ratio 1:2: n=42; ratio 1:4: n=38). Co-expression of P405L or I263T and the WT led to a significant reduction of the current amplitude compared to the WT alone. Groups were statistically different (One-way ANOVA ($p<0.001$), posthoc Dunn's method ($p<0.05$)). Shown are means ± SEM. **(E)** Western blot analysis from lysates of *Xenopus laevis* oocytes injected with equal amounts of $K_V1.2$-WT or mutant cRNA (P405L: top; I263T: bottom) or from lysates of CHO cells transiently transfected with $K_V1.2$-WT and P405L cDNAs (middle). For P405L-mutant channels there was a shift from 57 kDa to ~58.5 kDa (n=3). $K_V1.2$-WT or I263T (n=3) mutant channels revealed similar bands (57 kDa).

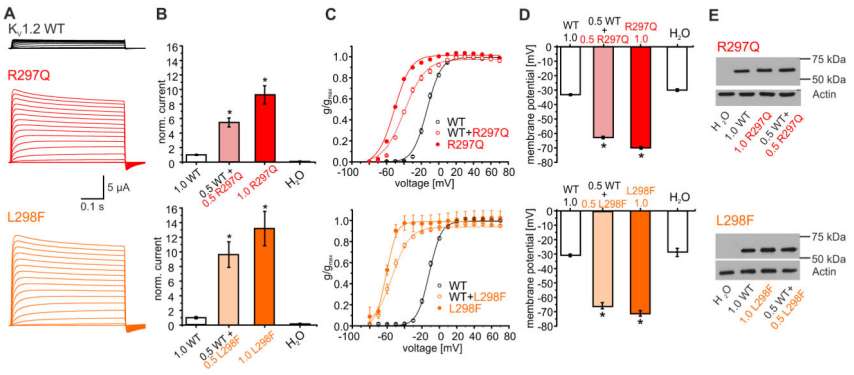

Figure 3.

Functional effects of the $K_V1.2$ mutations R297Q and L298F. **(A)** Representative current traces derived from $K_V1.2$-WT (top), R297Q (middle) or L298F mutant channels (bottom) recorded as described in Fig. 2A. **(B)** Mean current amplitudes of top: $K_V1.2$-WT (1.0, n=23), WT + R297Q (0.5:0.5, n=37), R297Q (1.0, n=35) and H_2O injection (n=25); bottom: $K_V1.2$-WT (1.0, n=13), WT + L298F (0.5:0.5, n=26), L298F (1.0, n=14), and H_2O injection (n=10). Shown are means±SEM. There was a statistical significant difference between WT and tested groups (ANOVA on ranks; $p<0.001$) with posthoc Dunn's Method ($p<0.05$)). **(C)** Mean voltage dependence of $K_V1.2$ channel activation for WT, R297Q (red, top) or L298F channels (orange, bottom). Shown are means ± SEM. Lines represent Boltzmann functions fit to data points. Activation curves of mutant channels were significantly shifted to more hyperpolarized potentials ($p<0.05$). For details see Supplementary notes. **(D)** Resting membrane potentials of oocytes injected with: top: WT (1.0, n=44), WT+R297Q (0.5:0.5, n=42), R297Q (1.0; n=38) or H_2O (n=24); bottom: WT (1.0, n=30), WT+L298F (0.5:0.5, n=34), L298F (1.0; n=28) or H_2O (n=13). Shown are means ± SEM. Statistically significant differences between WT and tested groups was verified by ANOVA on ranks ($p<0.001$) with posthoc Dunn's Method ($p<0.05$). **(E)** Western blot analysis from lysates of *Xenopus* oocytes injected with $K_V1.2$-WT (1.0), $K_V1.2$-WT (0.5) + R297Q (0.5, top), mutant R297Q (1.0, top), $K_V1.2$-WT (0.5) + L298F (0.5, bottom) or mutant L298F (1.0, bottom) cRNA (n=3). All channels revealed similar bands (57 kDa).

Table 1

Main phenotypic characteristics of patients carrying a disease-causing *de novo KCNA2* mutation.

	Patient 1	Patient 2	Patient 4	Patient 5	Patient 6	Patient 7
Cohort	1st epilepsy panel (n=33)	MAE (n=39)	DS (n=31)	adult EE I (n=147)	adult EE II (n=10)	Ataxia & epilepsy (n=12)
Mutation	c.1214C>T, p.Pro405Leu *de novo*	c.788T>C, p.Ile263Thr *de novo*	c.1214C>T, p.Pro405Leu *de novo*	c.1214C>T, p.Pro405Leu *de novo*	c.894G>T, p.Leu298Phe *de novo*	c.890G>A, p.Arg297Gln *de novo*
Functional consequence	loss of function				gain of function	
Gender/Age	F/8y	M/7y	F/5y	M/19y	M/36y	M/26y
Development prior to seizure onset	normal					
Age at seizure onset	17m	11m	10m	8m	6m	5m
Seizure type at onset	FS, hemiclonic seizures	MC	FS, FDS	Febrile SE	GTCS	Febrile SE
Other seizure types	FS, MC, FDS, focal motor seizures, secondary GTCS	MC, MA	FS, FDS, focal motor seizures, possible extension spasms	FS, focal motor seizures, secondary GTCS	MC, atypical absences	GTCS, absences
Seizure outcome	Seizure free since age 7 ½y old	Seizure free since age 4y old	Seizure free since age 4y old	Seizure free since age 15y old	GTCS bimonthly on polytherapy	GTCS once a year on lamotrigine
EEG at onset	Focal sharp waves	Focal sharp waves and spikes	normal	Sharp waves, bilateral centro-temporo-frontal spikes	n.a.	n.a.
Course of EEG	Multifocal sharp waves and sharp slow waves, accentuated over the left frontocentral region with significant increase during sleep	Multifocal sharp waves and polyspikes. Since age 6y: normal	Focal sharp waves. From age 2y: sharp waves, spike-waves and polyspike-waves over both centro-temporal regions, independently or bilaterally synchronous (left more than right); increase during sleep	At age 4y: multifocal epileptiform discharges activated by sleep Since age 17y: normal	At age 22y: frequent generalized spike wave discharges in a diffusely slow background	At age 6y: generalized spike waves and polyspike-waves
Neurological examination	Mild-moderate ataxia, constant myoclonus	normal	Mild ataxia, myoclonus at rest in hand and fingers	normal	Moderate ataxia, occasional myoclonus at rest	Moderate-severe ataxia, hyperreflexia
Development at last follow up	Mild-moderate ID, delayed speech development	Mild-moderate ID	Learning disability, delayed speech development	Moderate ID, delayed speech development	Severe ID, no speech, requires help with all aspects of daily activities	Moderate ID
MRI	normal					
Additional features	GH deficiency, IGF-1: −0.7 SDS (1y2m), −8.5 SDS (3y5m) subclinical hypothyroidism			Severe scoliosis	Facial dysmorphism (broad forehead, bulbous nasal tip, deep set eyes, synophris, full lips)	

Abbreviations: F: female; FDS: focal dyscognitive seizures; FS: febrile seizures; GH: growth hormone; GTCS: generalized tonic-clonic seizures; ID: intellectual disability; HC: head circumference; m: months; M: male; MA: myoclonic-atonic seizures; MC: myoclonic seizures; n.a.: not available; SE: status epilepticus; y: years